Proc. CIBSE A: Building Serv. Eng. Res. Technol. **19**(1) 15–21 (1998) Printed in Great Britain B448

Summary A computational fluid dynamics code has been used to model buoyancy-driven displacement ventilation flows. The results of using two eddy viscosity turbulence models are compared with those of mathematical theory and salt bath experiments carried out at the University of Cambridge. The work highlights some of the difficulties involved in modelling buoyancy-driven flows and identifies a preferable turbulence model for predicting such flows.

Buoyancy-driven displacement ventilation flows: Evaluation of two eddy viscosity turbulence models for prediction

M J Cook MSc GIMA and **K J Lomas** BSc PhD CEng MCIBSE MInstE
Institute of Energy and Sustainable Development, De Montfort University, Leicester LE1 9BH, UK

Received 24 March 1997, in final form 9 September 1997

List of symbols

C_p Specific heat capacity at constant pressure (J kg^{-1}K^{-1})
g_i, g Acceleration due to gravity (m s^{-2})
H_e Specific enthalpy (J kg^{-1})
k Turbulent kinetic energy (m^{2}s^{-2})
p Pressure (Pa)
S_ϕ Source term
T Temperature (K)
T_{Bref} Buoyancy reference temperature (K)
u_i u,v (velocity components in x and y directions) (m s^{-1})
x_i x, y (Cartesian coordinate system) (m)
β Thermal expansion coefficient (K^{-1})
δ_{ij} $\begin{cases} 1 \text{ if } i = j \\ 0 \text{ otherwise} \end{cases}$
ε Rate of dissipation of turbulent kinetic energy (m^2 s^{-3})
ϕ Arbitrary variable
$\Gamma_{s\phi}$ Diffusion coefficient
λ Thermal conductivity (W m^{-1}K^{-1})
μ Dynamic (laminar) viscosity (kg m^{-1}K^{-1})
μ_T Turbulent viscosity (kg m^{-1}s^{-1})
μ_{eff} $\mu + \mu_T$ (kg m^{-1}s^{-1})
r Density (kg m^{-3})
ρ_{Bref} Buoyancy reference density (kg m^{-3})
σ_{He} Turbulent Prandtl number for H_e
σ_k Turbulent Prandtl number for k
σ_ε Turbulent Prandtl number for ε

1 Introduction

There is a growing interest in the natural ventilation of buildings rather than mechanical ventilation or full air conditioning. One form of natural ventilation is buoyancy-driven displacement ventilation in which fresh air enters the space at low level, is drawn upwards in thermal plumes produced by equipment and occupants, and is then exhausted through high-level openings. This flow often causes stratification where warm, stale air rises above fresh, ambient air. It is the layer of warm, buoyant air that drives the flow through the openings. Designers are now turning to computer-based simulation tools to predict how naturally ventilated buildings might perform.

One such tool is computational fluid dynamics (CFD) programs. CFD is now well established in many fields of engineering, providing satisfactory solutions to a wide range of problems including building ventilation. An area where confidence needs to be increased is the modelling of buoyancy-driven flows. These are notoriously difficult to model for the following reasons: small driving forces lead to numerical instabilities; there is uncertainty regarding how to model turbulence accurately; and the flow is specified implicitly (i.e. sources of buoyancy are specified from which the program must calculate a velocity field). The first and last reasons mean that the user of a CFD code must exercise great care in controlling the iteration procedure to ensure that a solution is obtained. Techniques used to achieve this often make solving buoyancy-driven flows time-consuming.

This paper addresses the CFD modelling of a line source of buoyancy in a simple rectangular space using two different eddy viscosity turbulence models. The simulation results are compared with theoretical solutions and with experimental results obtained at the University of Cambridge[1]. It can be deduced from the Cambridge work that careful modelling of the plume produced by the buoyancy source is of paramount importance if the overall displacement ventilation flow is to be modelled accurately. The purpose of this work was to determine which, if any, of the turbulence models used was capable of modelling the buoyant plume reliably.

2 Theoretical and experimental work

The mathematical theory for displacement ventilation was derived and then verified experimentally by Linden *et al.*[1]. The work showed that in a space containing constant sources of buoyancy and openings to the exterior (ambient) fluid, steady states are possible (Figure 1).

The heat source produces a rising plume which entrains fresh (ambient) air taking it upwards into the upper region of the space where it is recirculated. As more and more light air accumulates in the upper region of the space, the rising plume begins to entrain this lighter air until a steady-state is achieved (Figure 1) in which a constant interface forms (at $y = h$) separating the dense, ambient air below the interface from the lighter, buoyant air above. In the steady state, the layer of warm, buoyant air drives a flow through the upper openings since the hydrostatic pressure difference between the top and bottom of the layer is smaller inside the space than between the same heights outside the space. Fresh air is then drawn in through the lower openings.

This flow is driven purely by buoyancy forces which result from differences in density $\Delta\rho$. Such forces can be thought of as reducing the gravity force g by an amount $g' = g\Delta\rho/\rho_0$ where ρ_0 is some reference density.

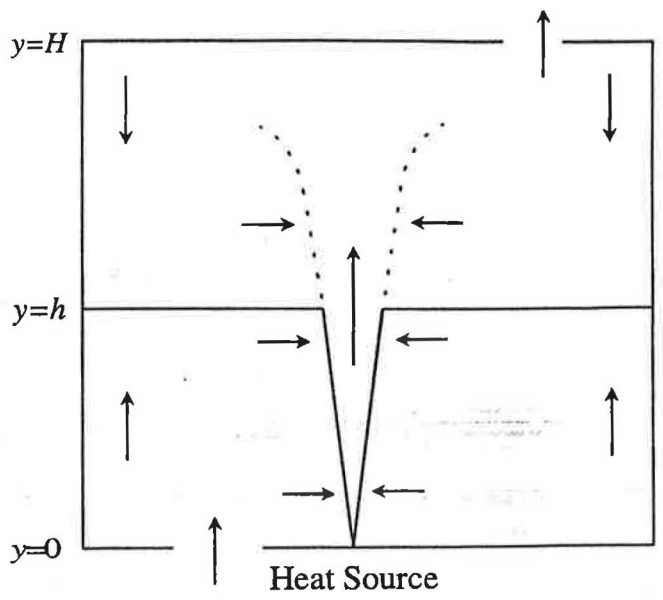

Figure 1 Steady displacement flow in a box containing a constant heat source (arrows show direction of flow), after Linden *et al.*[1]

A displacement ventilation flow can be defined by establishing expressions for the interface height and the *strength* of this stratification. The latter can be represented by the change in the buoyancy force g' across the interface which is due to a density change $\Delta\rho$ caused by a change in temperature ΔT:

$$g' = g\,\Delta\rho/\rho_0 = g\beta\,\Delta T \tag{1}$$

where the reference density ρ_0 is taken to be that of the ambient (incoming) air and β is the coefficient of thermal expansion.

The work of Linden *et al.*[1] used the plume assumptions of Morton *et al.*[2] as follows: (*a*) 'Top-hat' profiles were adopted for velocity and buoyancy (i.e. their values were taken to be constant inside the plume and zero outside). (*b*) Entrainment into the plume u was related to the velocity in the plume v through the *entrainment constant* α where $u = \alpha v$ ($\alpha \approx 0.1$). (*c*) The flow is incompressible. (Density differences are small.)

From the basic equations of plumes derived by Morton *et al.*[2], Linden *et al.*[1] equated buoyancy and volume fluxes through the lower openings with those in the plume at the interface level. This gave the following expressions relating interface height, stratification strength and opening areas for a line source of buoyancy:

$$A_L^*/H = 2\alpha[(h/H)^3/(1-h/H)]^{1/2} \tag{2}$$

$$g'/G_H' = H/h \tag{3}$$

where A_L^* is an effective opening area per unit length of the source defined as

$$A_L^* = a_u a_l/[1/2(a_u^2/c + a_l^2)]^{1/2} \tag{4}$$

where a_u is the total area of upper openings per unit length of the source, a_l is the total area of lower openings per unit length of the source and c is the momentum theorem constant (= 1 throughout this work).

G_H' is the (hypothetical) value of the reduced gravity of an ideal plume (in which $\alpha = 0.1$), if it were to reach $y = H$, and is given by

$$G_H' = B_L^{2/3}/H(2\alpha)^{2/3} \tag{5}$$

where B_L is the strength of the buoyancy source per metre along its length. This relates to a heat source of W_L watts per unit length as follows:

$$B_L = g\beta W_L/\rho C_p \tag{6}$$

The experimental work used the salt-bath modelling technique in which perspex models were placed upside down in a large tank of fresh water and brine injected to simulate the effects of a heat source. By applying various scaling laws[1] velocities and g' values measured in the brine experiments can be used to predict what would happen in air at full scale.

The Cambridge work drew the following important conclusions:

(*a*) The interface height is independent of the source strength (equation 2).

(*b*) The interface height increases as the areas of the openings increase (equation 2).

(*c*) The change in buoyancy across the interface decreases as the areas of the openings increase (equations 2 and 3).

(*d*) The change in buoyancy across the interface increases as the source strength increases.

3 The CFD package

The CFD package used for this work was CFX-F3D[3] version 4.1. This is a multiblock code in which geometries are defined using one or more topologically rectangular blocks. Each block is then covered with a mesh and the governing equations solved using the finite-volume method[4].

3.1 The governing equations

The code solves the conservation equations for mass, momentum and energy (enthalpy):

$$(\partial/\partial x_j)(\rho u_j\phi) - (\partial/\partial x_j)(\Gamma_\phi\,\partial\phi\partial x_j) = S_\phi \tag{7}$$

The source terms and diffusion coefficients are given in Table 1 for the variable ϕ. All transient terms have been omitted since the work sought steady-state solutions.

Table 1 Terms in the governing equations when using an eddy viscosity turbulence model

Conservation equation	ϕ	Γ_ϕ	S_ϕ
Mass	1	0	0
Momentum	u_i	$\mu+\mu_T$	$(\partial/\partial x_j)(-p_0\delta_{ij} + \mu_{eff}\partial u_j\partial x_i) + \rho g_i$
Enthalpy	H_e	$\lambda/C_p + \mu_T/\sigma_{He}$	0

p_0 is a 'modified' pressure given by

$$p_0 = p + {}^2/_3\rho k - \rho_{Bref} g_i x_i \tag{8}$$

Turbulence was modelled using two different eddy viscosity models. The first was the standard k–ε model[5] in which transport equations for k and ε are solved as follows:

$$(\partial/\partial x_j)(\rho u_j k) - (\partial/\partial x_j)[(\mu+\mu_T/\sigma_k)\partial k/\partial x_j] = P + G - \rho\varepsilon \tag{9}$$

$$(\partial/\partial x_j)(\rho u_j \varepsilon) - (\partial/\partial x_j)[(\mu+\mu_T/\sigma_\varepsilon)\partial\varepsilon/\partial x_j] = C_1(\varepsilon/k)P - C_2\rho\varepsilon^2/k \tag{10}$$

where $C_1 = 1.44$ and $C_2 = 1.92$ are empirical constants. P and G are production terms due to shear stresses and buoyancy respectively:

$$P = \mu_{eff}(\partial u_i/\partial x_j)(\partial u_i/\partial x_j + \partial u_j/\partial x_j)$$

and

$$G = (\mu_{eff}/\sigma_T)\beta g_j \partial T/\partial x_j$$

σ_T is the turbulent Prandtl number for k or ε depending upon which equation is being considered.

The second was the more recent renormalisation group (RNG) k–ε model[6]. This model assumes the same form of the k and ε equations but uses RNG theory to calculate the constants. This gives a more fundamental set of constants and eliminates the empiricism of the standard k–ε model. The constants are represented in CFX-F3D as follows.

C_1 is replaced with $C_1 - C_{1RNG}$ where

$$C_{1RNG} = \eta(1 - \eta/\eta_0)/(1 + \beta_1\eta_3)$$

$$\eta = (P/\mu_T)^{1/2}k/\varepsilon$$

$$\beta_1 = 0.015 \text{ and } \eta_0 = 4.38.$$

In both models the eddy viscosity is calculated using

$$\mu_T = \rho C_\mu k^2/\varepsilon$$

where

$$C_\mu = \begin{cases} 0.09 \text{ (standard } k\text{–}\varepsilon \text{ model)} \\ 0.085 \text{ (RNG } k\text{–}\varepsilon \text{ model)} \end{cases}$$

Buoyancy is modelled using the Boussinesq approximation[7] in which density is assumed to be constant except in the momentum equation where it is written

$$\rho = \rho_{Bref}[1 - \beta(T - T_{Bref})]$$

This gives rise to the buoyancy term in the modified pressure p_0 in Table 1.

All the governing equations are discretised using hybrid differencing (except the mass conservation equation where central differencing is always used), and solved on a co-located grid. Pressure and velocity are coupled using the SIMPLEC technique with the Rhie-Chow[8] interpolation algorithm to prevent decoupling due to the co-located grid. The following (default) under-relaxation factors were used: mass 1.0; momentum 0.65; enthalpy 1.0; k 0.7; and ε 0.7.

3.2 Boundary conditions

Three types of boundary condition were used in this investigation: WALL boundaries, PRESSURE boundaries and SYMMETRY PLANE boundaries.

WALL boundary conditions are placed at fluid–solid interfaces and enable the specification of velocities (normally zero), heat fluxes and temperatures. Conventional wall functions are imposed at WALL boundaries[4].

Fluid may flow into or out of the domain across a PRESSURE boundary. If fluid flows into the domain, Neumann conditions (i.e. zero normal gradient) are imposed on velocity and turbulence quantities, and values are assigned directly to pressure and temperature (Dirichlet conditions). When fluid flows out of the domain across a PRESSURE boundary, Dirichlet conditions are imposed on pressure, and Neumann conditions on all other variables.

At SYMMETRY PLANE boundaries, all variables are set to be mathematically symmetric, except the component of velocity normal to the boundary which is anti-symmetric.

4 Cases modelled

This paper considers air flow in a two-dimensional slice of a room (Figure 2). There are two upper openings, each with area a_u and two lower openings each with area a_l. The space is symmetrical about a vertical line through its centre, and the flow is driven by a constant heat source in the centre of the floor. The ambient temperature was 18°C and the flow was assumed to be incompressible. The governing equations modelled heat transfer by convection (and diffusion) only, i.e. radiative effects were ignored.

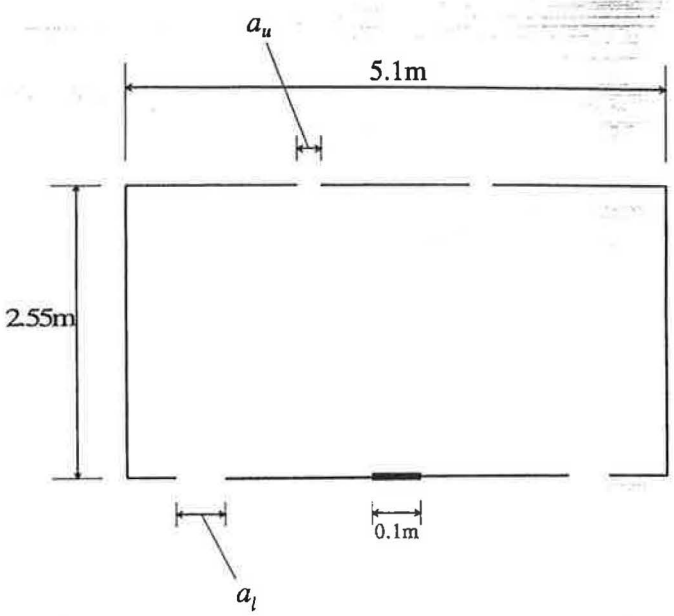

Figure 2 Geometry of space under consideration

The effects of varying the source strength and the opening areas were investigated.

5 CFD representation of the problem

It was deduced that a pressure boundary was required between the interior and exterior. However, it was thought necessary to model some of the exterior domain so that the detailed physics of the flow passing through the openings could be accounted for. In reality, the external air is unbounded, which is, of course, impossible to model literally. Consequently, a PRESSURE boundary was placed at some (finite) distance away from the room (Figure 3). The distance had to be estimated in an attempt to represent a pressure boundary 'at infinity', i.e. so that the boundary had no effect on the flow inside the room. It should be noted that in doing this, it was not the intention accurately to predict the flow in the exterior space.

Since in incompressible flows pressure is arbitrary to within an additive constant, and the hydrostatic pressure difference is automatically accounted for in the momentum equation (section 3.1), the value of p imposed at the PRESSURE boundaries could be set to a constant ($p = 0$). In order to reduce computational time and force a symmetrical flow, only half of the domain was modelled (Figure 3).

In order to define a two-dimensional slice, SYMMETRY PLANE boundaries were also specified on each plane face of the one-

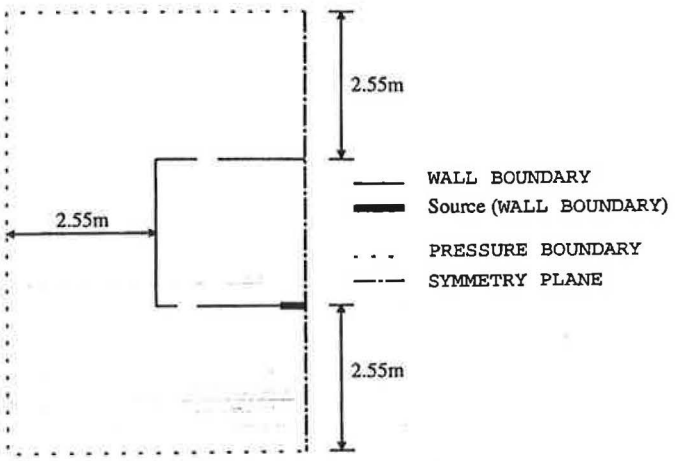

Figure 3 Geometry and boundary conditions used in the simulations

cell-thick slice. The distance between these two faces is arbitrary and was set to 1 m. The value of the heat flux imposed at the source is therefore the amount of heat emitted per square metre, for every metre length of the source in the z direction (perpendicular to the page).

6 Results

6.1 *Achieving convergence*

Convergence was deemed to have been reached when: (*a*) the enthalpy residual was less than 1% of the total heat entering the domain; and (*b*) the absolute values at some user-defined monitoring point did not change by more than about 0.1% over about 20 iterations.

In the simulations reported here, these convergence criteria could not be met using the default under-relaxation factors. The under-relaxation factors were therefore 'tightened' (reduced) in an attempt to control the convergence further, but the criteria were still not met.

As an alternative to reducing the under-relaxation factors, false time-stepping can be imposed on any of the governing equations. This implicitly specifies a more physical under-relaxation factor for that equation which reflects more closely the time scale over which that particular variable changes. It was found that by imposing false time-steps of 0.1 s on the two momentum equations, both convergence criteria could be met.

Imposing any form of under-relaxation (including false time-steps) has the effect of slowing down convergence, since the amount by which a variable changes between iterations is reduced. It is therefore cheaper (shorter simulation times) to run with 'looser' under-relaxation (i.e. no false time-stepping) for say 2000 iterations, and then to restart the simulation using the false time-steps for another 2000 iterations, say, rather than using false time-steps from the start. This was the approach used for the first simulation reported in this paper. All subsequent simulations were conducted using the previous result as an initial guess to the flow field, and used false time-steps of 0.1 s on the momentum equations.

6.2 *Qualitative results*

Results for all cases showed a flow pattern as predicted by the Cambridge work (see Figures 4–9). A plume formed above the heat source, warm air was forced out through the upper openings after some recirculation, and fresh air entered through the lower openings. A clear interface formed across which there was a sharp change in temperature and very little vertical flow.

Both turbulence models verified the qualitative conclusions of the Cambridge work (section 2): the interface height was independent of the source strength (Figures 4–7); the strength of the stratification (indicated by ΔT across the interface) increased with source strength (Figures 4–7); and as the opening areas increased, the interface rose and the stratification weakened (Figures 8 and 9). Figures 8 and 9 show the results for the RNG k–ε model, but the same effects were observed using the standard k–ε model.

A slight rise in the interface level was observed as the source strength was increased when using the RNG model. This is thought to be because this model predicted a narrower plume (cf Figures 5 and 7) which is more sensitive to the larger downward velocities impinging on its edge and opposing its upward progression than is the wider plume. It is hoped that such effects will be eliminated in three-dimensional simulations when the two-dimensional openings ('slots') can be modelled as 'holes'.

6.3 *Quantitative results*

The height of the interface was measured at the far left-hand side of the box (away from the plume and the incoming air), and was defined as that height at which there was least vertical motion. The stratification strength g' was measured using the change in enthalpy across the interface ΔH_e:

$$g' = (g\beta/C_p)\Delta H_e \qquad (11)$$

Both turbulence models gave favourable results for the reduced gravity across the interface g'/G_H' (Figure 10) but discrepancies existed between the two models regarding the interface height (Figure 11). The discrepancy is thought to be due to the RNG model predicting a narrower plume, which results from a smaller value of the entrainment into the plume. Equation 2 can be used to show that this produces a higher interface.

7 Conclusions

This work has shown that a commercial CFD code is able to predict simple two-dimensional displacement ventilation flows driven by buoyancy. However, special care was required in the control of the iteration process to ensure that a converged solution was attained. In the simulations reported here, false time-steps of 0.1 s were imposed on the two momentum equations.

Although both turbulence models were able to give good qualitative predictions of the flow, it has been verified that great care must be exercised in modelling the plume which is fundamental to the overall flow field in a displacement ventilation regime. The standard k–ε turbulence model demonstrated an inability to model entrainment into the plume accurately, and therefore gave discrepancies in the interface height as compared with the theory. In contrast, the RNG k–ε model predicted a narrower plume (due to less entrainment) resulting in a much closer agreement. The strength of the stratification is predicted fairly well using both turbulence models.

The slight discrepancies that still exist are thought to lie in the analytical solution where the discharge coefficient at the upper opening was not considered. It is also possible that the

RNG k–ε model is still slightly overpredicting entrainment into the plume, although it is a significant improvement on the standard k–ε model.

Acknowledgements

This work forms part of MC's PhD work undertaken at De Montfort University. The authors acknowledge advice from Dr G Whittle (Simulation Technology Ltd.) and Dr P Linden (University of Cambridge).

References

1 Linden P F, Lane-Serff G F, and Smeed D A Emptying filling boxes: the fluid mechanics of natural ventilation *J. Fluid Mech.* **212** 309–335 (1990)

2 Morton B R, Taylor G I and Turner J S Turbulent gravitational convection from maintained and instantaneous sources *Proc. R. Soc. London* **A234**(1) 1–23 (1956)

3 *Computational Fluid Dynamics Services CFX 4.1 Flow Solver User Guide* (Harwell: AEA) (1995)

4 Versteeg H K and Malalasekera W *An introduction to computational fluid dynamics — the finite volume method* (New York: Longman) (1995)

5 Launder B E and Spalding D B The numerical computation of turbulent flows *Computer Methods in Applied Mechanics and Engineering* **3** 269–289 (1974)

6 Yakhot V, Orszag S A, Thangham S, Gatski T B and Speziale C G Development of turbulence models for shear flows by a double expansion technique *Phys. Fluids A* **4**(7) 1510–1520 (1992)

7 Turner J S *Buoyancy effects in fluids* pp 165–206 (Cambridge University Press) (1973)

8 Rhie C M and Chow W L Numerical study of the turbulent flow past an airfoil with trailing edge separation *American Inst. Aeronautics and Astronautics J.* **21**(11) 1527–1532 (1983)

A vector length equal to the height of the space corresponds to a speed of 1.82 m s^{-1}.

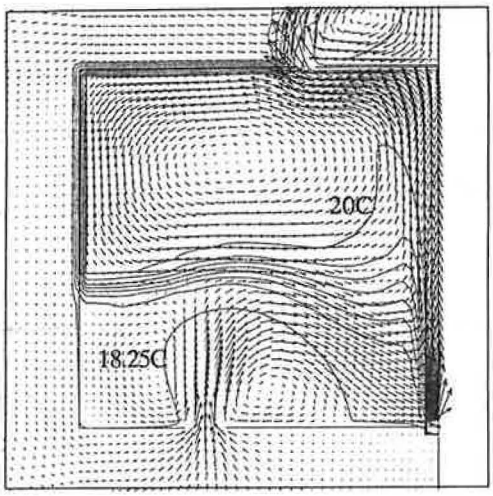

Figure 4 Flow pattern predicted using standard k–ε turbulence model (total heat input = 200 W, $A_L^*/H = 0.148$)

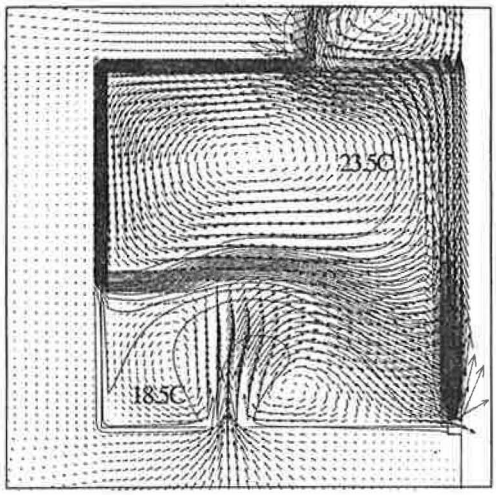

Figure 5 Flow pattern predicted using standard k–ε turbulence model (total heat input = 1000 W, $A_L^*/H = 0.148$)

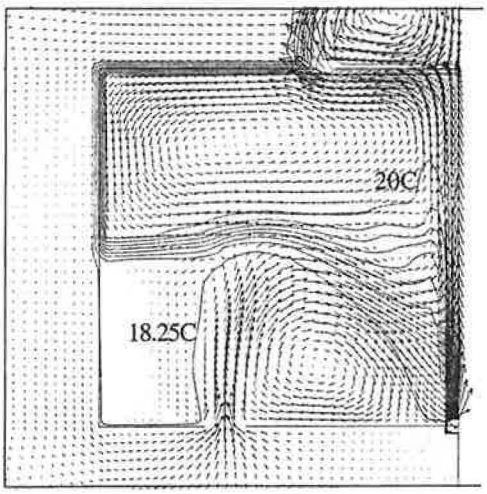

Figure 6 Flow pattern predicted using RNG k–ε turbulence model (total heat input = 200 W, $A_L^*/H = 0.148$)

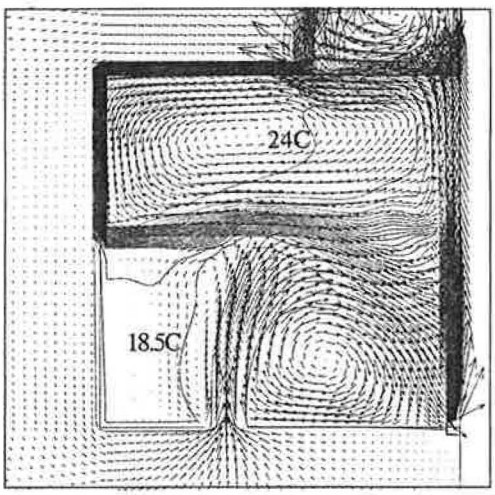

Figure 7 Flow pattern predicted using RNG k–ε turbulence model (total heat input = 1000 W, $A_L^*/H = 0.148$)

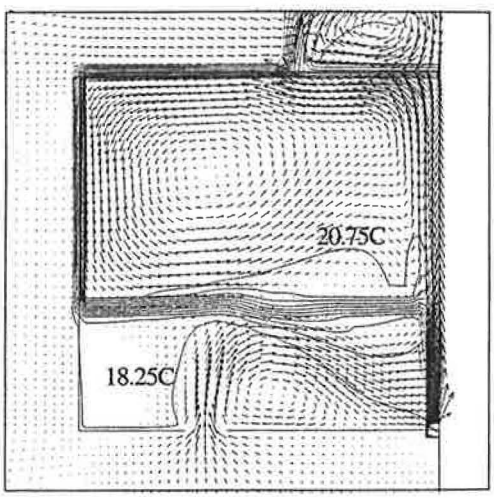

Figure 8 Flow pattern predicted using RNG k–ε turbulence model (total heat input = 200 W, $A_L^*/H = 0.075$)

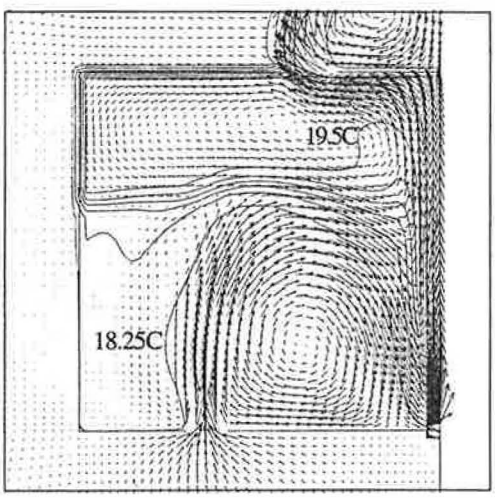

Figure 9 Flow pattern predicted using RNG k–ε turbulence model (total heat input = 200 W, $A_L^*/H = 0.227$)

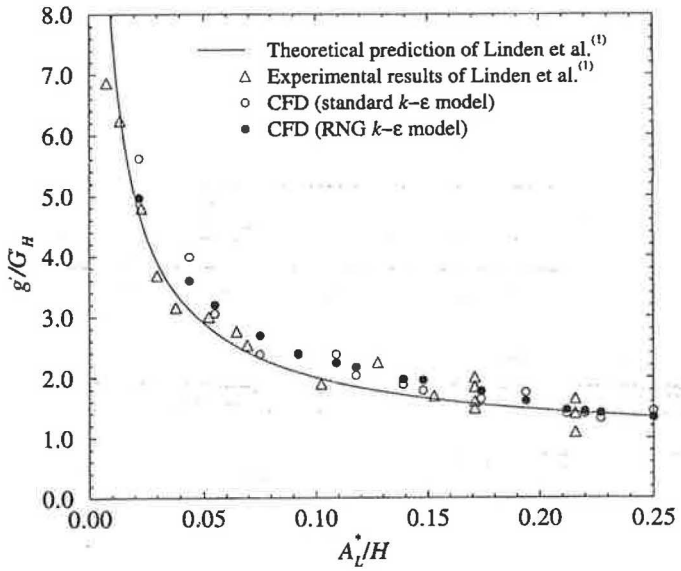

Figure 10 Reduced gravity across the interface for varying opening sizes (total heat input = 200 W)

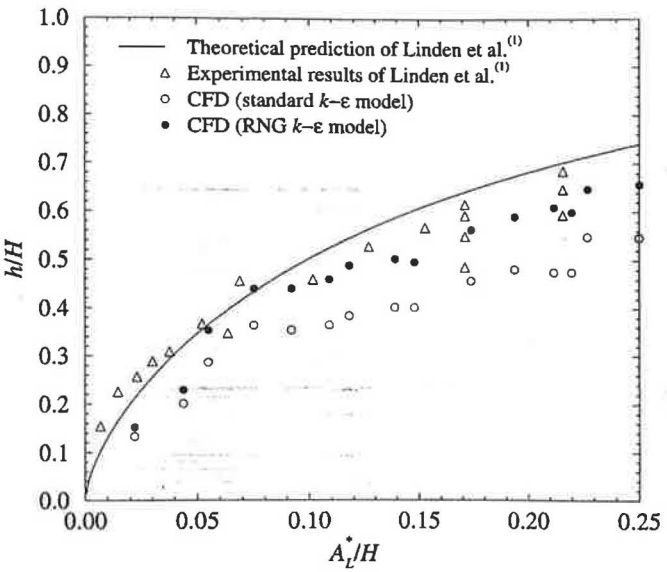

Figure 11 Interface height for varying opening sizes (total heat input = 200 W)